The binding site for an inhibitor of squalene:hopene cyclase determined using photoaffinity labeling and molecular modeling

Tongyun Dang, Ikuro Abe*, Yi Feng Zheng and Glenn D Prestwich

Background: The squalene:hopene cyclases (SHCs) are bacterial enzymes that convert squalene into hopanoids, a function analogous to the action of oxidosqualene cyclases (OSCs) in eukaryotic steroid and triterpenoid biosynthesis. We have identified the binding site for a selective, potent, photoactivatable inhibitor of an SHC.

Results: SHC from *Alicyclobacillus acidocaldarius* was specifically labeled by [^{3}H]Ro48-8071, a benzophenone-containing hypocholesteremic drug. Edman degradation of a peptide fragment of covalently modified SHC confirmed that Ala44 was specifically modified. Molecular modeling, using X-ray-derived protein coordinates and a single point constraint for the inhibitor, suggested several geometries by which Ro48-8071 could occupy the active site.

Conclusions: A covalent complex of a potent inhibitor with a squalene cyclase has been characterized. The amino acid modification and molecular modeling suggest that Ro48-8071 binds at the junction between the central cavity and substrate entry channel, therefore inhibiting access of the substrate to the active site.

Address: Department of Medicinal Chemistry, The University of Utah, 30 South 2000 East, Room 201, Salt Lake City, Utah 84112-5820 USA.

*Present address: School of Pharmaceutical Sciences, University of Shizuoka, 52-1 Yada, Shizuoka 422-8526, Japan.

Correspondence: Glenn D Prestwich
E-mail: gprestwich@deans.pharm.utah.edu

Key words: active-site mapping, benzophenone, enzyme inhibitor, triterpene biosynthesis

Received: **1 February 1999**
Revisions requested: **23 February 1999**
Revisions received: **4 March 1999**
Accepted: **10 March 1999**

Published: **6 May 1999**

Chemistry & Biology June 1999, **6**:333–341
http://biomednet.com/elecref/1074552100600333

 ISSN 1074-5521

Introduction

Oxidosqualene cyclases (OSCs) and squalene:hopene cyclases (SHCs) [EC 5.4.99.7] are pivotal enzymes in triterpenoid biosynthesis [1]. OSCs cyclize 2,3-oxidosqualene (OS) into lanosterol in fungi and mammals, and into cycloartenol and a variety of pentacyclic triterpenes in plants. Lanosterol and cycloartenol are then transformed into a medley of steroids that serve numerous roles, including stabilizing lipid bilayers by regulating membrane fluidity, functioning as hormones or feedback regulators of cholesterol homeostasis, and acting as meiosis-activating factors [2,3]. Hypercholesterolemia is a major risk factor for the development of atherosclerotic vascular diseases, and modulation of serum cholesterol with hypocholesteremic drugs has been shown to decrease the risk of cardiovascular disease [4]. Statins, a family of HMG-CoA reductase inhibitors that are currently used as cholesterol-lowering drugs, could, in principle, suppress all post-mevalonate biosynthetic pathways [4]. A preferred approach would be selective inhibition of OSC, as this would uniquely suppress the committed step in sterol biosynthesis.

In prokaryotes, squalene is converted by SHCs into pentacyclic triterpenoids (Figure 1), which have several functions analogous to those of eukaryotic steroids [5]. The first cloned and overexpressed SHC was obtained from the thermoacidophile *Alicyclobacillus acidocaldarius* [6]. Subsequently, SHC genes in *Zymomonas mobilis* [7], *Methylococcus capsulatus* [8] and *Bradyrhizobium japonicum* [9] have been cloned and expressed, and conserved hopanoid modification genes were cloned from an *shc* operon in *Z. mobilis* and *B. japonicum* [10]. The SHC genes from these species share 48–70% identity among their predicted protein sequences. Although no SHCs (or OSCs) from human pathogens have yet been cloned, it is conceivable that SHC or OSC inhibitors may provide leads for new antibiotics.

A comparison of eukaryotic OSCs and prokaryotic SHCs reveals a 17–38% sequence homology between these classes of enzymes. Both cyclase classes have a highly conserved repeating motif rich in glutamine and tryptophan residues (the QW repeat) [11,12], and an acidic-rich domain [13] that has been implicated in catalysis [14,15]. It is now believed that cyclization proceeds through a series of discrete conformationally rigid, partially cyclized carbocationic intermediates, either via a 'chair–boat–chair' or 'chair–chair–chair' conformation for OS, or via the all prechair conformation for squalene (Figure 1) [1,16]. Computational studies support the near-concerted manner of the formation of the A ring with electrophilic epoxide opening [17,18], and recent experimental evidence suggests the occurrence of a Markovnikov-like formation of a five-membered C-ring followed by rearrangement to the six-membered C-ring prior to completion of the tetracyclization by

Figure 1

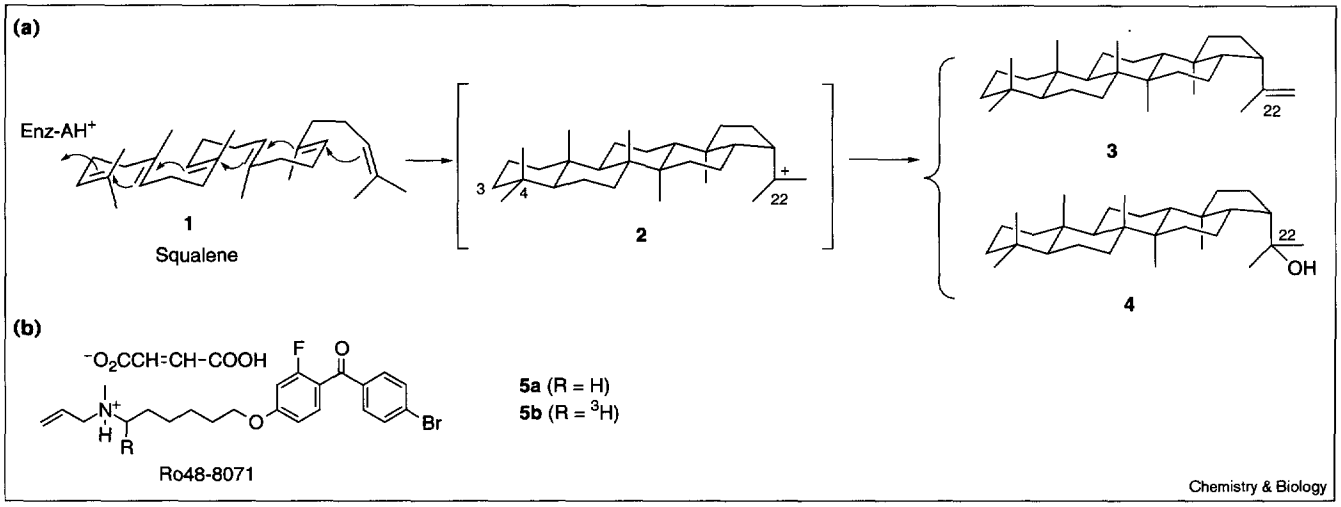

(a) The proposed mechanism for the cyclization of squalene (**1**) to hop-22-ene (**3**) and hopan-22-ol (**4**) by SHC. The ratio of **3**:**4** can vary from 4:1 to 16:1 under various enzymatic cyclization conditions. **(b)** The structure of the photoactivatable inhibitor Ro48-8071 (**5**).

OSC [19–21]. Similarly, pentacyclization by SHC appears to proceed through a five-membered ring intermediate en route to the hopanoid six-membered D-ring [22]. Following polycyclization, rearrangement and deprotonation of the protosteryl C-20 cation (for OS as substrate) or deprotonation of the C-22 cation (for squalene as substrate) yields cyclization products. The specific labeling of the carboxylate form of Asp456 in rat OSC by [^{3}H](3*S*)-29-methylidene-2,3-oxidosqualene (29-MOS), a mechanism-based irreversible inhibitor, implicated an essential function for Asp456 in stabilization of the C-20 carbocation [23]. Site-directed mutagenesis of Asp376 and Asp377 of SHC, the residues homologous to Asp456 and Cys457 of rat OSC, showed that both are crucial for catalysis [14].

We have reported previously [24] the efficient and specific labeling of both rat OSC and SHC by [^{3}H]Ro48-8071 (**5b**; Figure 1), a photoactivatable benzophenone (BP)-containing compound developed at Hoffmann-La Roche as an orally bioavailable pharmaceutical agent for lowering serum cholesterol levels [25]. We report here the identification of the amino acid residue of SHC that is photocovalently modified by Ro48-8071. On the basis of this result and the published crystal structure of SHC complexed to an amine N-oxide detergent molecule [26], two alternative binding conformations of the inhibitor in the catalytic cavity were predicted by molecular modeling. These results led us to propose a mode of action for the inhibitor that is consistent with its location in the entrance channel of the catalytic site.

Results

Recombinant SHC was expressed and purified as described previously [6,24]. In order to have a sufficient mass of labeled peptide fragments for sequence analysis, photoaffinity labeling was conducted in two stages. Homogeneous SHC was first photoaffinity labeled (45 min, 4°C, 360 nm) with [^{3}H] Ro48-8071 (**5b**) at an inhibitor concentration equivalent to 50% of its IC_{50} value. This accomplished efficient modification, generally >90% incorporation of radiolabel, with the high-specific-activity radioligand. A second labeling under the same conditions was then conducted with a threefold molar excess (3 μM) of unlabeled Ro48-8071 (**5a**) relative to the SHC concentration. As reported previously, we observed that [^{3}H] Ro48-8071 specifically labeled the SHC leading to a single radiolabeled band on a fluorogram of proteins separated using sodium dodecyl sulfate–polyacrylamide gel electrophoresis (SDS–PAGE) [24].

An aliquot (20 μg) of [^{3}H]Ro48-8701-labeled SHC was then digested with CNBr in formic acid. After the CNBr digestion, a tritium-labeled peptide fragment appeared as a unique 3 kDa band on SDS–PAGE and in the corresponding fluorogram (data not shown). Electrophoretic transfer from the gel to PVDF membrane was unsuccessful, probably due to the hydrophobicity and size of the modified peptide. Separation of products was instead achieved by reverse-phase high-performance liquid chromatography (RP–HPLC), giving three radioactive fractions at 36, 40 and 44 min. To determine which fraction(s) contained the covalently modified peptide(s), either [^{3}H] Ro48-8071 alone or [^{3}H] Ro48-8071-labeled SHC prior to digestion was analyzed under the same HPLC conditions; radioactivity was observed in fraction 40 for the former and fraction 44 for the latter. Fraction 36 was therefore suspected to contain the labeled peptide.

Improved resolution was required prior to sequence analysis. Fractions 35 and 36 were therefore pooled and again subjected to RP–HPLC. Fraction 3501 (collection time of 35.01–35.25 min) showed the highest radioactivity, whereas fraction 3526 (35.26 min–35.50 min) showed 50% lower radioactivity. Edman degradation of fraction 3501 revealed two overlapping sequences, which could be deconvolved to a primary sequence beginning with EKIRR (using single-letter amino-acid code) and a secondary sequence beginning with EAEYVV. The primary sequence (EKIRR...) corresponded to an anticipated 42-residue CNBr fragment peptide with a calculated mass of 4880.2 Da starting with Glu62 (cleavage at Met61). The secondary sequence (EAEYV...) corresponded to a 19-residue peptide starting with Glu43 (cleavage at Met42) with a calculated mass of 2346.6 Da (without ligand). Edman degradation of fraction 3476 (34.76–35.00 min) also showed the primary sequence EKIRR..., although this fraction lacked radioactivity, suggesting that this primary sequence was not from the [^{3}H]Ro48-8071-labeled peptide. Similarly, Edman analysis of the lower radioactivity fraction 3526 confirmed the presence of the EAEYVV... sequence, establishing that the peptide starting with Glu43 is indeed the labeled CNBr fragment of SHC. The eluted phenylthiohydantoin (PTH) amino acid derivatives obtained during the Edman degradation of fraction 3501 were monitored by liquid scintillation counting (LSC; Figure 2); only the second cycle showed significant radioactivity during the 30 cycles of Edman sequencing. On the basis of these results, we concluded that Ala44 was the specifically labeled amino acid residue.

To examine further the location and orientation of the noncompetitive inhibitor Ro48-8071 in the SHC active site, we used molecular modeling in conjunction with the X-ray structure coordinates for the published three-dimensional structure of SHC [26]. The modeling methods follow standard protocols [27,28], and include minimization of the protein structure prior to docking to accommodate hydrogen atoms not included in the crystal structure coordinates [29]. After generating a solvent-accessible surface on SHC using the Connolly algorithm [30] with H_2O molecules (radius = 1.4 Å), Ro48-8071 was manually docked into SHC with the BP carbonyl oxygen constrained to be within 3.0–5.0 Å of Ala44, while monitoring docking energy to achieve a minimum value. This constraint was imposed as a result of the photoaffinity-labeling experiment, which fixes the distance between the BP carbonyl and abstracted C–H bond to be within 3.1 Å [31].

Two positions of Ro48-8071 were found to have the lowest docking energy. In one position, the tertiary amine of Ro48-8071 points towards Trp489 (Figure 3a; orientation I); in the other position, the tertiary amine points towards Trp169 (Figure 3b; orientation II). The docked structures were first subjected to energy minimization and

Figure 2

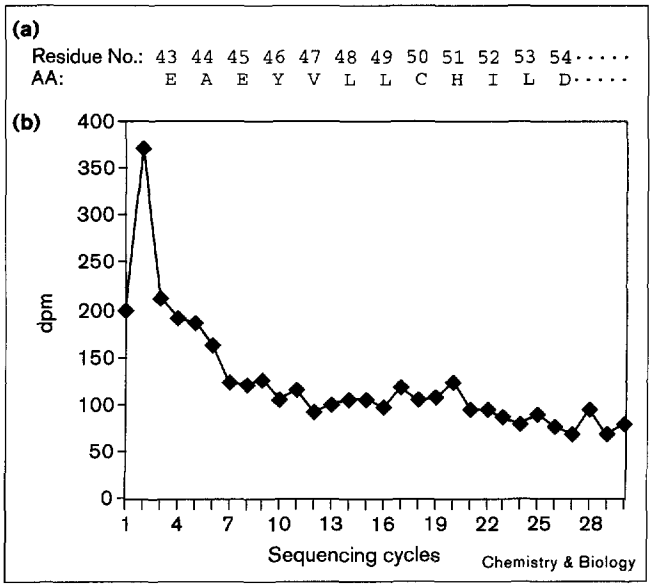

(a) Amino acid sequencing and **(b)** radioassay for fraction 3501 of [^{3}H]Ro48-8071-labeled SHC peptide after CNBr digestion.

then to dynamic simulations as described in the Materials and methods section. During energy minimization, the nonbonded repulsion energy was greatly decreased, presumably as a result of allowing the initially rigid conformation of the ligand to avoid direct clashes with amino acid residues in the active site. The BP oxygen was predicted to be close to the Glu45 carboxylate group, particularly in the average structure of the dynamics simulation for orientation II (Figure 3b), thus suggesting that Glu45 could be implicated in stabilization of a cationic cyclization intermediate. The labeling of Ala44 by the BP moiety of Ro48-8071 echoes this expected orientation; the known propensity of the BP diradicaloid species to abstract hydrogen from C–H bonds, particularly methyl or Cα hydrogens, would rationalize the labeling of Ala44 rather than Glu45 [31].

Figure 4a illustrates the calculated solvent-accessible surface of the SHC active-site cavity unoccupied by an inhibitor molecule. Figure 4b shows a view of the energy-minimized structure of orientation I of Ro48-8071 in this solvent-accessible cavity. Two hydrogen bonds between the protein and the inhibitor were predicted for this orientation. The overall root mean square deviation (rmsd) for backbone atoms between the minimized structure and crystal structure was 1.46 Å. One hydrogen bond was predicted between the BP carbonyl oxygen and Glu45 amide hydrogen (3.16 Å), whereas the other was between the Ro48-8071 aryl fluorine atom and the Gln262 amide hydrogen (3.07 Å). No hydrogen bonds for the flexible amine end of Ro48-8071 were predicted, although the

Figure 3

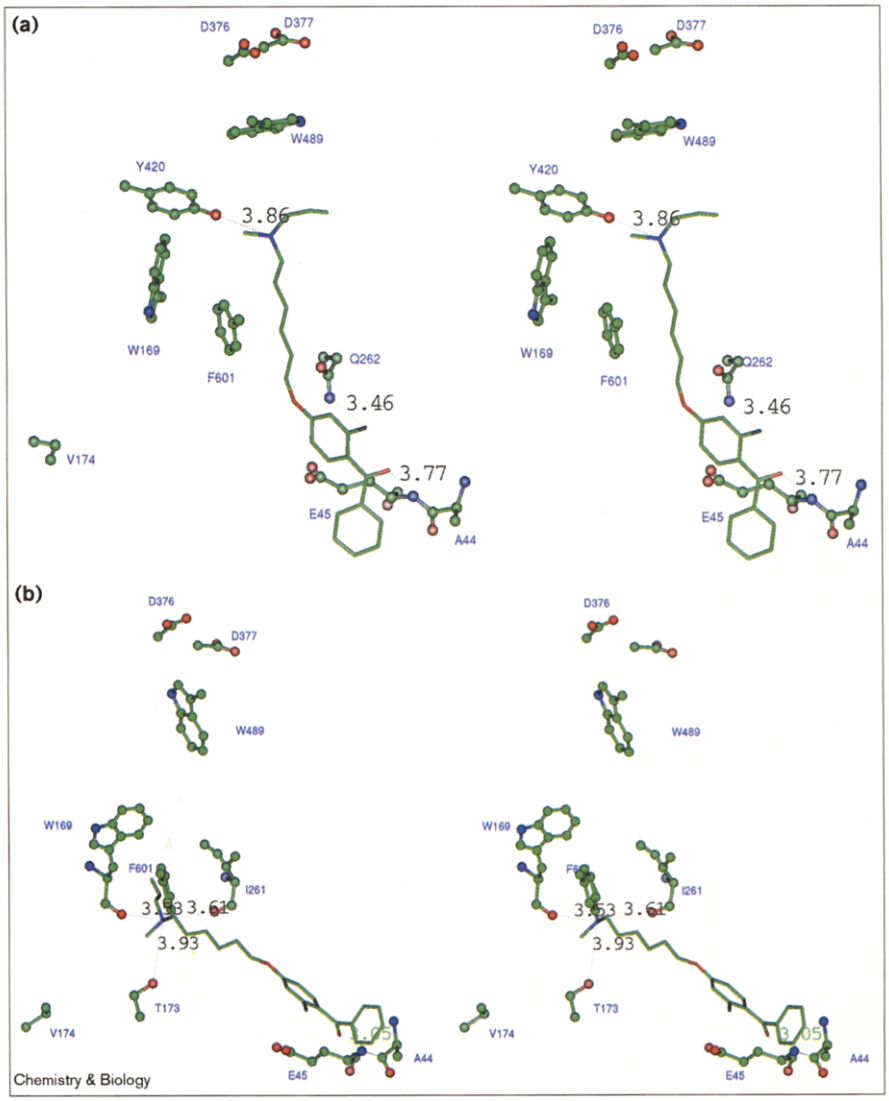

Stereopairs illustrating predicted average structures for dynamics simulations for two minimum-energy orientations of the Ro48-8071–SHC complex. **(a)** Orientation I. No hydrogen bonds were predicted. Several residues (e.g. Val174, Asp376 and Asp377) do not appear to be involved in the positioning of the Ro48-8071 inhibitor, but are shown as an aid in orienting the molecule for comparison with other published structural data [26,44]. **(b)** Orientation II. A hydrogen bond is predicted between the BP oxygen and the Glu45 amide hydrogen. The tertiary amine of Ro48-8071 might be stabilized by interactions with amide carbonyl groups of Ile261 and Trp169.

protonated tertiary amine might be stabilized by Tyr420 (3.75 Å). No hydrogen bonds were predicted for the average structure following the dynamics simulation (Figure 3a).

The energy-minimized structure for orientation II (Figure 4c) predicted that the BP carbonyl oxygen would move closer to Glu45 and Ala44, especially in the average structure of dynamics simulations (Table 1). The rmsd for backbone atoms between the minimized and crystal structures was 1.48 Å for this orientation; this value is essentially identical to the value for orientation I. The BP oxygen was closer to A44CB than to A44CA, suggesting the possibility that the methyl group (Cβ) instead of the Cα of Ala44 might be the site of covalent modification. No hydrogen bonds were predicted between the BP group and SHC. The protonated tertiary amine hydrogen was predicted, however, to form a hydrogen bond with the Thr173 hydroxyl group (distance of 2.93 Å). In addition, the protonated tertiary amine might also be stabilized by the Trp169 backbone carbonyl group (3.41 Å). In the average structure obtained from the dynamics simulation, a hydrogen bond was predicted between the BP carbonyl oxygen and the Glu45 backbone amide hydrogen (3.05 Å; see Figure 3b). Although the hydrogen bond between Thr173 and tertiary amine of Ro48-8071 was absent, the protonated amine still appeared to interact with amide carbonyl groups from Ile261 and Trp169 (distances of 3.61 Å and 3.53 Å, respectively; Figure 4b). During the molecular dynamics simulation, Ro48-8071 remained at approximately the same location as that determined in the energy-minimized structure, therefore implicating formation of a stable complex with SHC. This constant location was also observed for orientation I.

Figure 4

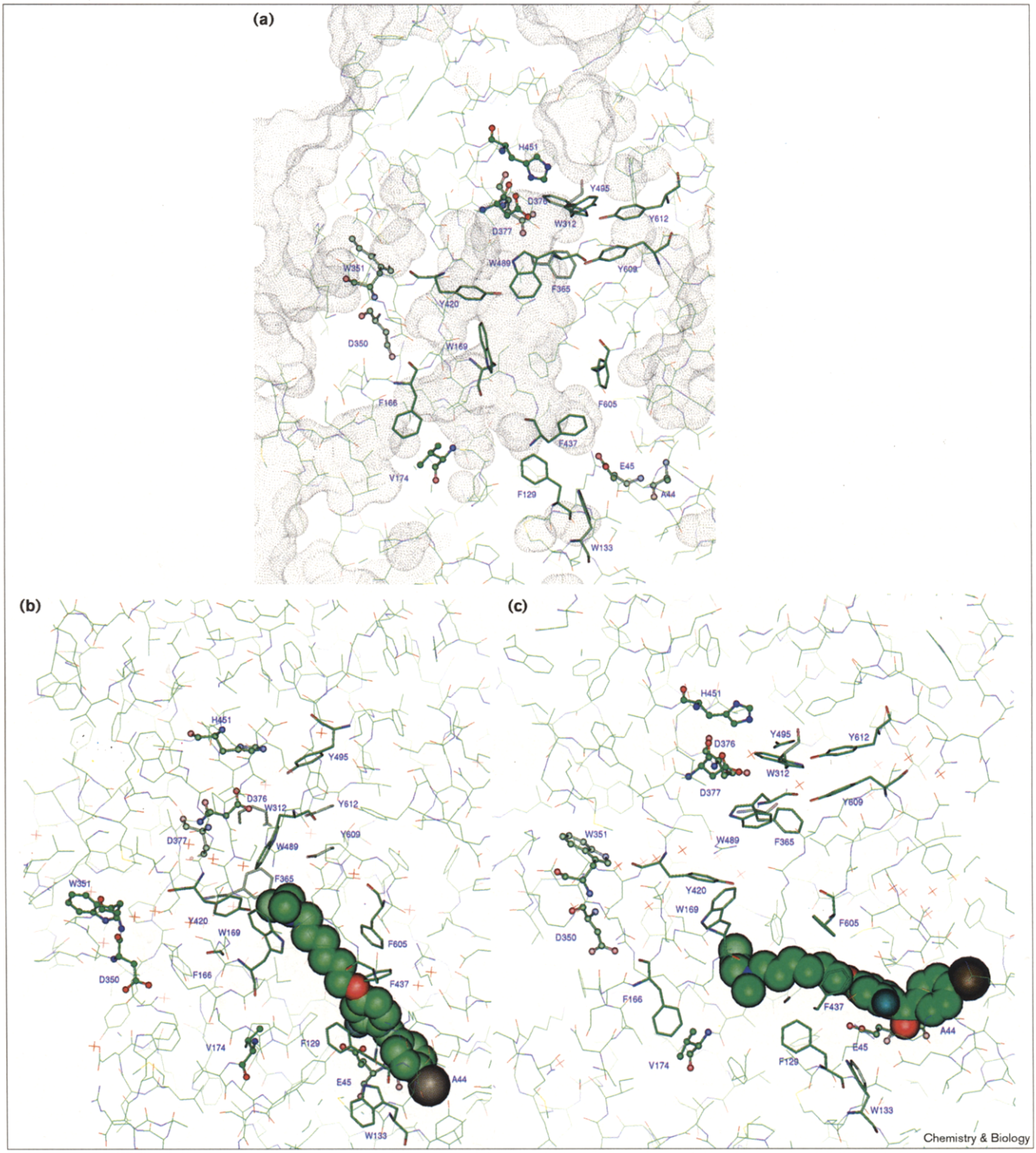

The active site of SHC. **(a)** The calculated solvent-accessible surface (generated using a water molecule as the probe) is shown in dot contour. All aromatic residues lining the active-site cavity are numbered and the sidechains are shown. The central cavity is between Asp376 and Glu45. The postulated channel for squalene entrance is represented by Val174. Another possible hydrophobic channel can be seen near the upper part of the figure as indicated by His451. **(b)** The cavity occupied by a space-filling model of Ro48-8071 in energy-minimized orientation I. **(c)** The cavity occupied by a space-filling model of Ro48-8071 in energy-minimized orientation II. The red crosses in (b) and (c) represent crystallographically defined water molecules.

Table 1

Calculated distances between the Ro48-8071 BP carbonyl oxygen and selected SHC atoms.

	Orientation I			Orientation II		
	Starting	Minimized	Dynamics	Starting	Minimized	Dynamics
BP→45CD (Å)	3.48	4.64	4.89	4.67	4.15	3.66
BP→A44CA (Å)	3.91	4.39	4.79	2.78	4.53	3.79
BP→A44CB (Å)	4.62	4.86	4.57	3.62	3.82	3.77
BP→N^+ (Å)	14.74	14.08	14.05	14.74	13.95	13.41

Distance of the structure before (starting) and after (minimized) the energy minimization, as well as the average structure of dynamics simulation (dynamics) are shown.

For both orientations I and II, Ro48-8071 adopted a semi-extended structure with a length of about 14 Å (Table 1). This compares well with the length of the pentacyclic intermediate (C-3 to C-22, 12.29 Å; Figure 1). Although the BP group was maintained close to Ala44 and Glu45 in both predicted orientations, the inhibitor locations differ considerably in the predicted position of the amino-terminal end, with the tertiary amine near Trp489 (Figure 3a) and Trp169 (Figure 3b). The primary constraint that was applied arose from the requirement that the hydrogen atom abstracted by the excited BP carbonyl oxygen radicaloid must be within 3.1 Å for any bimolecular chemistry to occur between the inhibitor and the protein [31]. The modeling appears to provide two principal solutions that are consistent with this requirement and with molecular considerations in the active site.

Discussion

The cyclization of OS by OSC, and by analogy the cyclization of squalene by SHC, is now believed to occur via a multistep process involving successive carbocationic intermediates [1,13,16,32]. Until recently, few details of protein structure were available that would lend credence to the hypothesized mechanisms [14,20,23,33]. It was proposed that an electrophilic residue would initiate the cyclization by protonating the terminal isopropylidene of squalene, or by opening the epoxide ring of OS. The identity of this residue was postulated to be Asp376 of SHC based on the three-dimensional structure with the detergent *N*,*N*-dimethyldodecylamine *N*-oxide (LDAO) [26] bound in the active site, and Asp456 for OSC based on mutagenesis and active-site modification studies [15].

To date, however, neither OSC nor SHC has been co-crystallized with a bound substrate- or product-like inhibitor. We therefore conducted a photoaffinity-labeling experiment with a potent inhibitor, Ro48-8071, to determine the precise location of the BP photophore in the active site. The BP moiety is unique among photoactivatable groups in one key regard: photocovalent attachment only occurs when the carbonyl group is constrained to be within 3.1 Å of a target C–H bond [31]. No reactive species would be produced, as would be the case for carbenes or nitrenes, that could diffuse away from the bound site and react non-specifically elsewhere with the protein or with solvent [34].

The solution of the three-dimensional structures of SHC and two sesquiterpene cyclases have led to the postulation of two separately evolved families of isoprenoid-cyclizing enzymes [35]. The theme of 'template, trigger, chaperone and sequester' [36] is maintained in both classes: the substrate first binds to the enzyme by adopting a specific 'product-like' conformation; second, the cyclase triggers cation formation by metal-assisted diphosphate dissociation (class I) or by protonation of an epoxide or a double bond (class II); third, the cyclase chaperones reactive carbocationic intermediates through sequential ring-closures and rearrangements; and finally, the terpene cyclases sequester and stabilize the cationic intermediates, preventing solvent access or interception by active-site nucleophiles [35,36]. Both the chaperoning and sequestration can now be seen to involve π-cation interactions, first discussed for metal cation and carbocation interactions with proteins by Dougherty [37], with sidechain aromatic rings.

The Hoffmann-La Roche team reported a series of BP-containing compounds as potent, orally active cholesterol-lowering agents that acted as inhibitors of OSC [38]. The inhibitory activity was dependent on the distance between the nitrogen atom of the tertiary amine and the carbonyl group of the BP moiety [25]. Ro48-8071 was indeed a potent noncompetitive SHC inhibitor [24], so its mode of action was likely to be important in understanding the cyclization process. Examination of both possible orientations of inhibitor binding (Figures 3 and 4) suggests that Ro48-8071 might inhibit SHC by binding at the intersection of the squalene entrance channel and the opening of the main central cavity. Two other structurally related classes of orally active aromatic, nonterpenoid OSC inhibitors were independently discovered at Boehringer Ingelheim Pharma KG [39,40]. These noncompetitive inhibitors might act in a structurally similar fashion to Ro48-8071, but their activity against SHC has not been examined in detail.

Analysis of a 2.9 Å resolution three-dimensional crystal structure of SHC showed that the enzyme crystallized as a

dimer. The structure revealed two α–α barrel domains that assemble to form a central hydrophobic cavity. These α-barrel domains are topologically distinct from the single α-helical bundles that characterize the two sesquiterpene cyclases [35]. Domain 1 is an α6–α6 barrel of two concentric rings of parallel helices, whereas domain 2 appears to have evolved from domain 1 by gene duplication and loss of one of the helices [26]. SHC has a central cavity of 1200 Å^3, in which the catalysis is presumed to take place. This cavity is lined with aromatic residues (e.g., Trp312, 133, 169, 489; Phe365, 605, 437, 129, 166; and Tyr612, 609, 495, 420); Asp376 and Asp377 are located at the top and Glu45 at the bottom of the cavity as illustrated in Figure 4. Two of these tryptophan residues, Trp169 and Trp489, appear to be important in the determination of cyclization termination [41]. SHC mutants Trp169→Phe, Trp169→His and Trp489→Phe each furnished a novel 6/6/6/5 tetracyclic dammarene product in which the hopene E ring failed to form and proton loss from the dammarenyl C-20 cation led to a 20(21)-methylene group.

The cavity can accommodate an extended squalene molecule, because the distance between the two carboxylate groups of Asp376 and Glu45 is 25.11 Å (24.85 Å in the minimized structure); the distance from C-2 and C-22 of squalene is 25.22 Å. Due to its location and the existence of a hydrogen bond between Asp374 and Asp377, Asp376 was proposed to protonate the terminal isopropylidene bond of squalene [26]. Termination of cyclization may occur near Glu45, probably due to steric hindrance. A water molecule near the hydrogen-bond network involving Gln262:Glu45:Glu93:Arg127 may stabilize or quench the C-22 carbocation [26]. Our results suggest that Glu45, which is highly conserved in the SHC sequences, could be the nucleophilic residue important in cyclization termination. As the major product of SHC is hopene (**3**) rather than hopanol (**4**), Glu45 rather than water may act as the stabilizing nucleophile. This role of Glu45 is also consistent with the preliminary studies on the site of covalent modification of SHC by the suicide substrate 29-MOS (T.D., I.A. and Y.F.Z., unpublished observations), and by the observation that no products were isolated from 29-MOS cyclization that would correspond to the quenching of cationic intermediate by water [42]. It is an unresolved paradox that the alkylation of Asp456 of rat OSC by the mechanism-based irreversible inhibitor 29-MOS implicated this residue as the putative 'negative point charge' [43] necessary for stabilization of the C-20 carbocation [23]. The resolution of this paradox will entail solving the structure of an SHC or OSC structure with either a complexed squalenoid substrate mimic or with a covalently attached mechanism-based inhibitor. In any event, the DCTAEA motif containing Asp456 is highly conserved for OSCs [13], whether it is involved in initiation or termination of the cyclization. For SHC, mutagenesis of either Asp376 or Asp377 of the homologous DDTAV motif to nonacidic residues resulted in loss of catalytic activity; moreover, even the more subtle Asp376→Glu and Asp377→Glu mutants had only 10% and 0.04% activity, respectively, compared with the wild-type enzyme [14].

The central cavity can be connected through a nonpolar channel to the surface SHC, where a nonpolar plateau of 1600 Å^2 was proposed to facilitate diffusion of the substrate squalene from the membrane [26]. The modeling results described here revealed a moderately hydrophobic channel close to His451 (Figure 4) not described in the original structure [26] but subsequently seen in a higher resolution crystal structure that was published during revision of this manuscript [44]. As this channel also has nonpolar residues on the surface facing outside, it could constitute an alternative for substrate entry, or possibly in permitting product release. Although SHC exists as a dimer in the presence of 0.3% C_8E_4 (*n*-octyltetraoxyethylene) under crystallization conditions, gel filtration shows that SHC appears to have a molecular weight of over 250–300 kDa in the absence of Triton X-100 (T.D. and I.A., unpublished observations). This may suggest SHC has more than one surface hydrophobic patch.

Significance

Squalene:hopene cyclase (SHC) is responsible for a templated and enzyme-initiated cationic polyolefinic cyclization of squalene to hopene. The sequence homology and well-conserved regions between SHCs and the eukaryotic oxidosqualene cyclases (OSCs) implicate the strongly conserved structural and mechanistic similarities. Analysis of an inhibitor complexed to the three-dimensional structure of SHC therefore provides an important insight into understanding the enzymatic reaction of OSC.

This is the first time that a covalently modified SHC residue has been identified. Using the site of modification as a distance constraint, molecular modeling was employed to demonstrate the occupancy of the central hydrophobic cavity by a cholesterol-lowering nonterpenoid analog. The blocking of the junction of the central cavity and the substrate entrance presumably accounts for the potency of Ro48-8071 as a noncompetitive inhibitor of both SHC and OSC. This knowledge may help in the design of more potent and selective inhibitors of OSC and SHC.

Materials and methods

Enzyme preparation and labeling

SHC from the acidothermophilic bacterium *A. acidocaldarius* was expressed in *Escherichia coli* and purified as described previously [6]. Briefly, membrane proteins were prepared from cell lysate by centrifugation and then solubilized in the presence of 1% Triton X-100. SHC was first separated by heat denaturation of *E. coli* proteins (60°C for 10 min); the enriched SHC was then purified by ion exchange on a DEAE-Sephacel column.

Purified SHC was quantified using the DC Protein Assay kit (Bio-Rad), and enzymatic activity was assayed at pH 6.0, 60°C using [^{14}C]-squalene as the substrate with a reaction buffer containing 100 mM sodium citrate and 0.1% Triton X-100. [^{3}H]Ro48-8071 was synthesized as described previously [24]. SHC was first photoaffinity labeled by [^{3}H]Ro48-8071 (a final concentration of 3 nM, 18.7 Ci/mmol), then photolabeled with unlabeled Ro48-8071 (threefold molar excess). Both photoaffinity-labeling reactions were performed by preincubation at 60°C in reaction buffer for 15 min, followed by UV irradiation (360 nm) for 45 min at 4°C.

Chemical and enzymatic cleavage

[^{3}H]Ro48-8071-Labeled SHC was divided into aliquots of 20 µg, concentrated and lyophilized using a Speed-vac, and digested overnight with CNBr (Sigma, 300-fold molar excess over methionine residues) in 70% formic acid under argon in darkness.

Peptide separation and sequencing

CNBr-digested, [^{3}H]Ro48-8071-labeled SHC fragments were separated by either 7.5% SDS–PAGE containing Tricine or RP–HPLC. SDS–PAGE was performed at constant current (10 mA), followed either by fluorography or by transferring to PVDF membrane (Millipore) under constant voltage of 50 V for 1 h. The gel was stained with 0.1% Coomassie Blue R-250, destained, washed with 100% acetic acid after destaining, impregnated with EN^{3}HANCE (NEN Life Science Products), miniaturized with 50% polyethylene glycol (PEG, 1450) and dried. The dried gel was exposed to X-ray film (Kodak X-Omat AR film) for 3–7 days at −80°C. PVDF membranes used for electrotransfer was briefly stained with Coomassie Blue R-250 and the radiolabeled fragment was sequenced by Edman degradation (ABI model 477). Radioactivity of sequencing eluates were counted by LSC.

For HPLC separation, a C_8 RP column (Whatman, 4.6 mm × 5 cm) was used with the following gradient: 0%–50% B for 30 min; 50%–100% for 60 min; 100% B for 10 min. Buffer A is 0.06% TFA in H_2O, and buffer B is 0.052% TFA in 80% acetonitrile. The flow rate was 1 ml/min and UV absorbance was monitored at 214 and at 280 nm. Fractions were collected at 200–250 µl each and counted by LSC. Radioactive fractions were then submitted for sequencing by Edman degradation.

Molecular modeling

The structure of SHC was downloaded from Brookhaven Database (identification code 1SQC) into INSIGHT II (Biosym Technologies, version 97). The ligand (LDAO) used for crystallization was removed, but crystallographic water molecules were retained during modeling. Hydrogen atoms were added using the software programs provided, and then allowed to move for 1000 steps, followed by minimization of the entire enzyme for 2000 steps using the method of steepest descents.

The ligand was built by the Builder module, energy minimized (CVFF force field) to energy derivatives of less than 0.1 kcal/Å, and manually docked into energy-minimized SHC, while monitoring the energy change using the Docking module. Energy minimization was first run for 2000 steps using steepest descents, followed by minimizing to the energy derivatives of less than 0.1 kcal/Å using the conjugate gradients method. Molecular dynamics ran for 10,000 iterations of 1 fs after 1000 steps of equilibration, while the distance between BP oxygen and the Cα-H of Ala44 was constrained to be 3.0–3.5 Å. All energy minimization and molecular dynamics, except calculation of ligand alone, were carried out at pH 6.0, temperature 333K, and cut-off distance of 15 Å with switching-function width of 1.5 Å. This temperature was selected to reflect the 60°C optimal temperature for the enzymatic reaction.

Acknowledgements

The authors are indebted to K. Poralla (Universität Tübingen) for the *A. acidocaldarius* SHC clone and R.W. Schackmann (The University of Utah, UU) for Edman peptide sequencing. We thank M.R. Ziebell (UU), F.G. Whitby (UU) and T. Poulos (University of California at Irvine) for assistance with molecular modeling and manuscript revision, and K.U. Wendt (University of California at Berkeley) for critical comments on this manuscript. Financial support was provided by the National Institutes of Health (Grant GM 44836 to G.D.P.).

References

1. Abe, I., Rohmer, M. & Prestwich, G.D. (1993). Enzymatic cyclization of squalene and oxidosqualene to sterols and triterpenes. *Chem. Rev.* **93**, 2189-2206.
2. Rodriguez, R.J., Low, C., Bottema, C.D. & Parks, L.W. (1985). Multiple functions for sterols in *Saccharomyces cerevisiae*. *Biochim. Biophys. Acta* **837**, 336-343.
3. Byskov, A.G., *et al.*, & Roed, T. (1995). Chemical structure of sterols that activate oocyte meiosis. *Nature* **374**, 559-562.
4. Abe, I., Tomesch, J.C., Wattanasin, S. & Prestwich, G.D. (1994). Inhibitors of squalene biosynthesis and metabolism. *Nat. Prod. Rep.* **11**, 279-302.
5. Seckler, B. & Poralla, K. (1986). Characterization and partial purification of squalene-hopene cyclase from *Bacillus acidocaldarius*. *Biophys. Biochim. Acta* **881**, 356-363.
6. Ochs, D., Kaletta, C., Entian, K.-D., Beck-Sickinger, A. & Poralla, K. (1992). Cloning, expression, and sequencing of squalene-hopene cyclase, a key enzyme in triterpenoid metabolism. *J. Bacteriol.* **174**, 298-302.
7. Reipen, I.G., Poralla, K., Sahm, H. & Sprenger, G.A. (1995). *Zymomonas mobilis* squalene-hopene cyclase gene (shc): cloning, DNA sequence analysis, and expression in *Escherichia coli*. *Microbiology* **141**, 155-161.
8. Tippelt, A., Jahnke, L. & Poralla, K. (1998). Squalene-hopene cyclase from *Methylococcus capsulatus* (Bath): a bacterium producing hopanoids and steroids. *Biophys. Biochim. Acta.* **1391**, 223-232.
9. Perzl, M., Muller, P., Poralla, K. & Kannenberg, E.L. (1997). Squalene-hopene cyclase from *Bradyrhizobium japonicum*: cloning, expression, sequence analysis and comparison to other triterpenoid cyclases. *Microbiology* **143**, 1235-1242.
10. Perzl, M., *et al.*, & Kannenberg, E.L. (1998). Cloning of conserved genes from *Zymomonas mobilis* and *Bradyrhizobium japonicum* that function in the biosynthesis of hopanoid lipids. *Biochim. Biophys. Acta* **1393**, 108-118.
11. Poralla, K. (1994). The possible role of a repetitive amino acid motif in evolution of triterpenoid cyclases. *Bioorg. Med. Chem. Lett.* **4**, 285-290.
12. Poralla, K., Hewelt, A., Prestwich, G.D., Abe, I., Reipen, I. & Sprenger, G. (1994). A specific amino acid repeat in squalene and oxidosqualene cyclases. *Trends Biochem. Sci.* **19**, 157-158.
13. Abe, I. & Prestwich, G.D. (1999). Squalene epoxidase and oxidosqualene:lanosterol cyclase. Key enzymes in cholesterol biosynthesis. In *Comprehensive Natural Products Chemistry*; (Barton, D.H.R. & Nakanishi, K., eds), in press.
14. Feil, C., Sussmuth, R., Jung, G. & Poralla, K. (1996). Site-directed mutagenesis of putative active-site residues in squalene-hopene cyclase. *Eur. J. Biochem.* **242**, 51-55.
15. Corey, E.J., Cheng, H.M., Baker, C.H., Matsuda, S.P.T., Li, D. & Song, X.L. (1997). Studies on the substrate binding segments and catalytic action of lanosterol synthase. Affinity labeling with carbocations derived from mechanism-based analogs of 2,3-oxidosqualene and site-directed mutagenesis probes. *J. Am. Chem. Soc.* **119**, 1289-1296.
16. van Tamelen, E.E. (1982). Bioorganic characterization and mechanism of the 2,3-oxidosqualene-lanosterol conversion. *J. Am. Chem. Soc.* **104**, 6480-6481.
17. Gao, D.Q., Pan, Y.K., Byun, K. & Gao, J.L. (1998). Theoretical evidence for a concerted mechanism of the oxirane cleavage and A-ring formation in oxidosqualene cyclization. *J. Am. Chem. Soc.* **120**, 4045-4046.
18. Jenson, C. & Jorgensen, W.L. (1997). Computational investigations of carbenium ion reactions relevant to sterol biosynthesis. *J. Am. Chem. Soc.* **119**, 10846-10854.
19. Corey, E.J. & Cheng, H.M. (1996). Conversion of a C-20 2,3-oxidosqualene analog to tricyclic structures with a five-membered C-ring by lanosterol synthase. Further evidence for a C-ring expansion step in sterol biosynthesis. *Tetrahedron Lett.* **37**, 2709-2712.
20. Corey, E.J., *et al.*, & Sarshar, S. (1995). New insights regarding the cyclization pathway for sterol biosynthesis from (*S*)-2,3-oxidosqualene. *J. Am. Chem. Soc.* **117**, 11819-11820.
21. Hoshino, T. & Sakai, Y. (1998). Further evidence that the polycyclization reaction by OSLC proceeds via a ring expansion. *J. Chem. Soc. Chem. Commun.* **1998**, 1591-1592.

22. Pale-Grosdemange, C., Feil, C., Rohmer, M. & Poralla, K. (1998). Occurrence of cationic intermediates and deficient control during the enzymatic cyclization of squalene to hopanoids. *Angew. Chem. Int. Ed.* **37**, 2237-2240.
23. Abe, I. & Prestwich, G.D. (1994). Active site mapping of affinity-labeled rat oxidosqualene cyclase. *J. Biol. Chem.* **269**, 802-804.
24. Abe, I., Zheng, Y.F. & Prestwich, G.D. (1998). Photoaffinity labeling of oxidosqualene cyclase and squalene cyclase by a benzophenone-containing inhibitor. *Biochemistry* **37**, 5779-5784.
25. Morand, O.H., *et al.*, & Himber, J. (1997). Ro 48-8071, a new 2,-oxidosqualene:lanosterol cyclase inhibitor lowering plasma cholesterol in hamsters, squirrel monkeys, and minipigs: comparison to simvastatin. *J. Lipid Res.* **38**, 373-390.
26. Wendt, K.U., Poralla, K. & Schulz, G.E. (1997). Structure and function of a squalene cyclase. *Science* **277**, 1811-1815.
27. DeSantis, G., Berglund, P., Stabile, M.R., Gold, M. & Jones, J.B. (1998). Site-directed mutagenesis combined with chemical modification as a strategy for altering the specificity of the S1 and S1′ pockets of subtilisin *Bacillus lentus*. *Biochemistry* **37**, 5968-73.
28. Sundaramoorthy, M., Terner, J. & Poulos, T.L. (1998). Stereochemistry of the chloroperoxidase active site: Crystallographic and molecular-modeling studies. *Chem. Biol.* **5**, 461-473.
29. Dauber-Osguthorpe, P., Roberts, V.A., Osguthorpe, D.J., Wolff, J., Genest, M. & Hagler, A.T. (1988). Structure and energetics of ligand binding to proteins: *Escherichia coli* dihydrofolate reductase-trimethoprim, a drug-receptor system. *Proteins* **4**, 31-47.
30. Connolly, M. (1993). The molecular surface package. *J. Mol. Graph.* **11**, 139-141.
31. Dormán, G. & Prestwich, G.D. (1994). Benzophenone photophores in biochemistry. *Biochemistry* **33**, 5661-5673.
32. van Tamelen, E.E. & James, D.R. (1977). Overall mechanism of terpenoid terminal epoxide polycyclizations. *J. Am. Chem. Soc.* **99**, 950-952.
33. Abe, I., Zheng, Y.F. & Prestwich, G.D. (1998). Mechanism-based inhibitors and other active-site targeted inhibitors of oxidosqualene cyclase and squalene cyclase. *J. Enzym. Inhib.* **13**, 385-398.
34. Prestwich, G.D., Dormán, G., Elliott, J.T., Marecak, D.M. & Chaudhary, A. (1997). Benzophenone photoprobes for phosphoinositides, peptides, and drugs. *Photochem. Photobiol.* **65**, 222-234.
35. Wendt, K.U. & Schulz, G.E. (1998). Isoprenoid biosynthesis: manifold chemistry catalyzed by similar enzymes. *Structure* **6**, 127-133.
36. Lesburg, C., Caruther, J., Paschall, C. & Christianson, D. (1998). Managing and manipulating carbocations in biology: terpenoid cyclase structure and mechanism. *Curr. Opin. Struct. Biol.* **8**, 695-703.
37. Dougherty, D.A. (1996). Cation-π interactions in chemistry and biology: a new view of benzene, Phe, Tyr, and Trp. *Science* **271**, 163-168.
38. Jolidon, S., Polak, A.-M., Guerry, P. & Hartman, P.G. (1989). Inhibitors of 2,3-oxidosqualene lanosterol cyclase as potential antifungal agents. *Biochem. Soc. Trans.* **18**, 47-48.
39. Mark, M., Muller, P., Maier, R. & Eisele, B. (1996). Effects of a novel 2,3-oxidosqualene cyclase inhibitor on the regulation of cholesterol biosynthesis in HepG2 cells. *J. Lipid Res.* **37**, 148-158.
40. Eisele, B., Budzinski, R., Muller, P., Maier, R. & Mark, M. (1997). Effects of a novel 2,3-oxidosqualene cyclase inhibitor on cholesterol biosynthesis and lipid metabolism *in vivo*. *J. Lipid Res.* **38**, 564-575.
41. Hoshino, T., Sato, T. & Abe, T. (1998). Cyclization mechanism of squalene: a ring expansion process of D-ring formed by Markovnikov closure, proved by site-directed mutagenesis and by using squalene analogue C-27 with hydroxyl group. *42nd Symposium on the Chemistry of Terpenes, Essential Oils, and Aromatics*. pp 266-268. Gifu, Japan.
42. Abe, I., *et al.*, & Prestwich, G.D. (1997). Cyclization of (3*S*)-29-methylidene-2,3-oxidosqualene by bacterial squalene:hopene cyclase: irreversible enzyme inactivation and isolation of an unnatural dammarenoid. *J. Am. Chem. Soc.* **119**, 11333-11334.
43. Johnson, W.S. (1991). Fifty years of research: a tribute to my co-workers. *Tetrahedron* **47**, xi-1.
44. Wendt, K., Lenhart, A. & Schulz, G. (1999). The structure of the membrane protein squalene-hopene cyclase at 2.0 Å resolution. *J. Mol. Biol.* **286**, 175-187.

Because *Chemistry & Biology* operates a 'Continuous Publication System' for Research Papers, this paper has been published via the internet before being printed. The paper can be accessed from http://biomednet.com/cbiology/cmb – for further information, see the explanation on the contents pages.